Switchable conductivity at the ferroelectric interface: Nonpolar oxides

Kurt D. Fredrickson and Alexander A. Demkov

Phys. Rev. B **91**, 115126 — Published 13 March 2015

DOI: 10.1103/PhysRevB.91.115126

Switchable conductivity at the ferroelectric interface: nonpolar oxides

Kurt D. Fredrickson and Alexander A. Demkov[1]
Department of Physics, The University of Texas at Austin, Austin, TX 78712, USA

We investigate theoretically the interface between a ferroelectric $BaTiO_3$ film and a non-polar insulating $SrTiO_3$ substrate. We find that thin $BaTiO_3$ (under 5 nm) can stabilize a non-polarized state, and an additional metastable polarized state. While the non-polarized state is insulating, for the polarized heterostructure, we discover the existence of two-dimensional charge carrier gases. In this case, the heterostructure undergoes an electronic reconstruction in order to prevent the polar catastrophe. The two-dimensional gases, formed as a result, screen the polarization, leading to a substantially reduced potential drop across the ferroelectric film. We emphasize that the two-dimensional electron and hole gases are created by the polarization of the sample, and are not due to polar nature of the material or to doping.

I. Introduction

The astounding discovery of a conducting layer at the interface of two large band gap, insulating oxides, $LaAlO_3$ (LAO) and $SrTiO_3$ (STO), by Ohtomo and Hwang[1] has led to an obvious question: how can the interface of two insulators be conductive? The answer is widely believed to be a phenomenon known as the polar catastrophe.[2–4] Left uncompensated, a large electric field is built-up in a polar oxide such as LAO; the alternating positively charged LaO and negatively charged AlO_2 layers lead to a ramping up of the electrostatic potential that grows without limit. Due to the large cost of the corresponding internal field, and to avoid dielectric breakdown, the heterostructure must do something to counter the polarization catastrophe. In many cases, atomic reconstruction is the solution, where diffusion of atoms or vacancies helps to reduce or eliminate the internal field.[5–10] Another way to avoid the polar catastrophe is electronic reconstruction, where the electronic charge migrates to the interface to eliminate the field. This interfacial charge density resulting from electronic reconstruction is often referred to as a two-dimensional electron gas (2DEG), due to its localization at the interface between LAO and STO.[5,8,11–13] The thickness of LAO is also an important factor; there is a critical thickness of LAO where the 2DEG forms and the interface undergoes an insulator-metal transition, with a critical thickness of four unit cells (UC) of LAO[14] for an LAO/STO structure and six UC's in LAO/STO multilayer structures.[15] It was also found that even when the LAO thickness is less than the critical thickness of 4 UC, the interface could still be made conducting by applying a gate voltage.[14] Theory has suggested that some of the electrons at the interface are localized in sub-bands and do not contribute to the conductivity,[16] explaining why experimentally the charge density measured is much lower than the expected 0.5e per unit cell.[6,7,14,17] Compressive strain has been shown to decrease the conductivity of the 2DEG and increase the critical LAO

[1] demkov@physics.utexas.edu

thickness for formation of the 2DEG; however, tensile strain was shown to result in an insulating interface.[18]

Experiment and theory show that the 2DEG at the oxide/oxide interface has many exotic features. It can be paramagnetic, ferromagnetic or even superconducting,[11,12,19,20] with strong Rashba splitting leading to a controllable magnetic moment.[21–23] Although the 2DEG is usually thought of as localized at the interface, the spatial extent of the gas has been found to vary from a depth of a few nanometers to hundreds of micrometers.[24] The varying spread of the 2DEG is due to many factors, including oxygen vacancy concentration,[24] temperature of the system,[7] charge density of the gas,[25] amount of cationic exchange,[26] and ionic relaxation at the interface.[27–29]

It has been demonstrated that various modifications of the LAO/STO heterostructure also lead to a variety of interesting effects. Arras *et al.* showed that adding a variety of metallic layers on LAO leads to an increase or decrease of the field in LAO, and in one case, even creating a spin-polarized 2DEG at the interface.[30] Although most of the experiments were done on LAO grown on bulk STO, there have also been reports of the 2DEG found in LAO/STO heterostructures deposited on Si, paving the way for semiconducting devices utilizing the properties of the oxide 2DEG.[31] Levy and co-authors used atomic force microscope lithography to induce a reversible metal/insulator transition of the interface.[32,33]

Although the discussion of 2DEGs is dominated by the STO/LAO interface, there are reports of 2DEGs being formed in a variety of other oxide materials. Even in pure STO, replacing a SrO layer with a rare earth-oxide (RO) ML leads to an additional donated electron in the system. Depending on the rare earth atom substituted, the ML can be either insulating, or a 2DEG may form.[34] Inserting sub-monolayer doping levels of La in pure STO induces a change from 3D to 2D conducting states, depending on the concentration of the La dopant levels.[35] 2DEGs have also been seen in heterostructures containing neither STO or LAO; theoretically, a $YMnO_3$/GaN heterostructure was shown to have a spin-dependent conduction band offset due to a spin-polarized metallic interface.[36] The combination of two polar materials ($Mg_xZn_{1-x}O$/ZnO) led to a 2DEG at the interface due to charge being driven there by the polarization of the materials; however, these materials are not switchable.[37]

There is evidence that ferroelectrics may allow for the creation of surface charge. In the bulk of a ferroelectric, the material cannot be metallic, due to screening of the polarization due to conduction electrons.[38] However, there is experimental and theoretical evidence of the formation of a two-dimensional conducting layer on the surface of clean ferroelectrics, which is attributed to the uncompensated surface charge due to the ferroelectric nature of the material.[39–43] A prior study has shown that a $PbZr_{0.2}Ti_{0.8}O_3$-$LaNiO_3$ heterostructure allows a switchable conduction layer at the interface, although in this case the substrate is already metallic.[44] In a recent theoretical study, Niranjan *et al.* have shown that the charge density at a polar ferroelectric

$KNbO_3$(KNO)/STO interface can change depending on the polarization state of the ferroelectric, due to variation in electronic screening of the polarization.[45] While the charge density of the 2DEG at the KNO/STO interface can be modified by switching the polarization of KNO (provided it is a single domain film), the origin of the 2DEG is in the polar nature of KNO, which is clear as the 2DEG is still seen even when KNO is in a paraelectric state with no polarization present. In other words, although the 2DEG responds to the change in the polarization of the sample, the polarization does not *create* the 2DEG. In fact, one thing that all prior work on 2DEGs at the interface of insulating oxides has in common is that the creation of the 2DEG is due to either a) the polar nature of one of the materials, or b) the addition of dopants to introduce extra electrons. In this paper, we propose that a 2DEG can be created at the interface of two insulating nonpolar oxides, one of which is ferroelectric. Crucially, neither of the materials is polar! That is, the 2DEG is *created* by the polarization of the system, which is seen by the fact that in the nonpolarized, paraelectric state, the entire system is insulating. Our goal is to study an interface of a stoichiometrically non-polar ferroelectric $BaTiO_3$ (BTO) with a "normal" band insulating oxide STO to determine the feasibility of creating a 2DEG purely via spontaneous polarization. We choose STO as it is commonly used as a substrate for epitaxial BTO growth;[46–48] the STO/BTO system is itself interesting due to theoretical reports of increased BTO polarization[49] and giant dielectric response.[50]

The rest of the paper is organized as follows. We describe the computational methods used in this work in section II. In section III, we discuss the structure and polarization stability. The appearance of a two dimensional conducting state at both the BTO/STO interface and at the BTO surface is discussed in section IV. We summarize our results in section V.

II. Computational Details

All calculations are done using density functional theory (DFT) within the local density approximation (LDA) and plane augmented-wave pseudopotentials as implemented in the VASP code.[51–56] We employ the Perdew-Zunger form of the exchange-correlation potential.[57] We use the valence configuration $3p^6 4s^2 3d^2$ for titanium, $5s^2 5p^6 6s^2$ for barium, $4s^2 4p^6 5s^2$ for strontium, and $2s^2 2p^4$ for oxygen. We use a 650 eV kinetic energy cutoff for all calculations. For the Brillouin zone integration, we use the following Monkhorst-Pack[58] k-point meshes: 8x8x8 for bulk BTO, 8x8x8 for bulk STO and 8x8x1 for the BTO/STO superstructures. Bulk BTO and STO are fully optimized, and all structures are optimized with respect to the ionic positions until the forces on all atoms are less than 10 meV/Å. For the BTO/STO superstructures we optimize the ionic positions until the forces are less than 30 meV. The energy is converged to 10^{-3} meV/cell. The relaxation is not constrained by symmetry.

We restrict our consideration to the cubic phase of STO, as this is the phase most commonly used in experimental growth. We calculate the lattice constant of STO to be 3.861 Å, in good

agreement with previously reported experimental value of 3.905 Å[59] and a theoretical value of 3.918 Å.[60] At high temperature BTO is cubic, but at 393 K it transforms to a tetragonal ferroelectric phase. As we are interested in the room temperature properties of BTO, we restrict ourselves to studying the tetragonal phase. Our calculated lattice constant *a* of 3.960 Å and c/a ratio of 1.005 compare favorably with the experimental values of a = 3.990 Å and c/a = 1.011,[61] and with previously reported theoretical values of a = 4.00 Å and c/a = 1.010.[62] As BTO has a larger lattice constant than STO, setting the lateral size of BTO to be that of STO results in a compressive strain of 2.5%.

To investigate the BTO/STO junction and comply with the periodic boundary conditions, we use a 6 unit cell thick STO layer representing a substrate, with two 10-unit-cell-thick BTO slabs attached on either side, each terminated with a TiO_2 layer; 15 Å of vacuum separates the slabs. We note that our BTO is ~4 nm thick, above the critical thickness for ferroelectricity of ~2.4 nm shown previously in literature for LDA.[63] The interface between the two materials is represented by a $BaO/TiO_2/SrO$ layer sequence (Figure 1). We allow all of the BTO and the first unit cell of STO on either side to relax; we freeze the central UC of STO to mimic the experimental conditions of a bulk substrate. To make sure that the vacuum is thick enough for our calculations, we examine the plane-averaged electrostatic potential and verify that the potential of the system reaches a constant value in the vacuum region.

III. Polarization Stability

To test the effect of polarization on the STO/BTO superstructure, we consider six different polarization configurations: no polarization (which we refer to as P_0), polarization with Ti atom moving away from the surface and toward the interface (which we refer to as P_+), and polarization with Ti moving toward the surface and away from the interface; we do all three cases with TiO_2-terminated and BaO-terminated BTO, for a total of six cases. The polarization of a unit cell of either BTO or STO is given by

$$P_\beta^* = \frac{1}{\Omega}\sum_\kappa \int Z^*_{\kappa,\alpha\beta} d\tau_{\kappa,\alpha} \tag{1}$$

where P is the polarization, Ω is the volume of the unit cell, τ is the displacement of the ion, κ indexes the ions in the unit cell, α, β are Cartesian directions, and Z* is the Born effective charge tensor given by

$$Z^*_{\kappa,\alpha\beta} = \Omega \frac{dP_\beta}{d\tau_{\kappa,\alpha}} \tag{2}$$

We calculate Z* using density functional perturbation theory.[64,65] As the change in polarization is highly linear with respect to the ionic displacement, as a very good approximation,[66] we calculate P by

$$P_\beta = \frac{1}{\Omega}\sum_\kappa Z^*_{\kappa,\alpha\beta}\tau_{\kappa,\alpha} \quad (3)$$

In bulk BTO, we find P to lie exclusively in the [001] direction with a value of 22.9 μC/cm^2, in reasonable agreement with previously reported experimental value of 27 μC/cm^2,[67] and a theoretical value of 30 μC/cm^2.[68] The rumpling, given by the relative displacement of the Ti and O ions, is calculated to be 0.096 Å in bulk. In the heterostructure, the calculation of polarization is somewhat less straightforward; due to relaxation effects, the unit cell volume is not constant for each layer of BTO or STO. The lateral strain is obviously the same for each unit cell of the same material as it is set by the periodic boundary conditions of the simulation cell, but the height (length in the c-direction) of each cell is allowed to vary and does relax into the vacuum. We define a cell be from one AO plane to the next AO plane (A=Ba,Sr). We calculate the rumpling as the difference in z-direction between Ti and O atoms in the TiO_2 plane and the difference in z-direction between Ba (Sr) and O in the BaO (SrO) planes. We use the bulk values of Born effective charges of STO and BTO for the heterostructures; for the TiO_2 layer at the interface, we use the average of the Ti and O Born effective charges of BTO and STO.

First we will examine the TiO_2-terminated structures. We find that the case of the polarization pointing toward the surface of BTO is unstable, and the system relaxes to the un-polarized paraelectric case. This appears to be due to the strong tendency of the surface TiO_2 plane to relax away from the vacuum (Ti atoms "sink" into the crystal).[69,70] The effect of the surface can be overcome if a much thicker BTO layer is used. However, in our calculation, a 180° domain wall would need to be considered, which in a previous work we calculated to have an energy 0.11 J/m^2.[71] The full examination of this problem is beyond the intended scope of this paper. The rumpling and polarization are shown in Figure 2 for both stable structures, one where the polarization points away from the BTO surface and towards the BTO/STO interface (the P_+ case), and another where the BTO is un-polarized (the paraelectric P_0 case). We see that the P_+ case retains just under half the polarization and rumpling of the bulk. We also find that the P_0 configuration is lower in energy than the P_+ by 20 meV per cell at this thickness. Upon examining the BaO-terminated heterostructures, we see that all three polarization states relax to the un-polarized, paraelectric state, giving us a total of three unique polarization states; TiO_2-terminated, polarized away from the surface (P_+); TiO_2-terminated, un-polarized (P_0); and BaO-terminated, un-polarized. Although we have shown that it is only possible to obtain two states for the heterostructure with the TiO_2-terminated surface (polarized away from the surface, or unpolarized),the addition of a metallic capping layer may allow the BTO to polarize away from the interface; indeed, our prior calculations have shown that 5 ML of Pt as a capping layer for 10

UC of BTO is enough to stabilize ferroelectricity.[71] The addition of a metallic capping layer could also protect the surface from unwanted adsorption by foreign material.

We also examine the Ti-O bond lengths of the interface for the three heterostructures; for reference, the bulk STO bond Ti-O bond length is 1.93 Å, and in BTO there are two Ti-O bond lengths in the c-direction due to the rumpling of the TiO_2, with 1.87 Å being the shorter bond length and 2.11 Å being the longer bond length. Upon examining the Ti-O bond lengths at the interface, we see that in the P_0 case, the Ti-O bond length for the O in the BaO layer is 2.03 Å, and the Ti-O bond length to the O in the SrO layer is 1.93 Å; the in-plane Ti-O bond length is 1.93 Å. The Ti-O bond length for the SrO layer is the same as bulk STO, and the Ti-O bond in the BaO layer is between the that of STO and the long bond length in BTO. The difference in bond length for the BaO layer is due to the strain of BTO being lattice matched to STO. In the P_+ heterostructure, the Ti-O bond length for the O in the BaO layer is 2.09 Å, and the Ti-O bond length to the O in the SrO layer is 1.96 Å; the in-plane Ti-O bond length is 1.93 Å. The differing bond lengths are due the small but nonzero rumpling of the TiO_2 layer. The bond lengths for the BaO-terminated heterostructure are essentially the same as those of the P_0 case.

We also examine the plane-averaged electrostatic potential of the P_+ and P_0 configurations and compare them in Figure 3. One can see that there is a noticeable change in potential in the polarized portion of BTO, as is expected; however, we see that the potential is also noticeably different in the STO. We note that the difference in potential energy at the center of the slab is approximately 0.81 eV, with the P_0 case being higher. This suggests that on an insulating substrate, the change in potential in the substrate should be measureable between a polarized and non-polarized film. The change in potential is due to the electric field resulting from the polarization of BTO. Averaging over BTO, we get a polarization of 16.45 μC/cm^2; assuming a constant polarization P in BTO of this value and relative permittivity of free space ($\varepsilon_r = 1$), the magnitude of the electric field E is

$$E_{BTO} = \frac{P}{\varepsilon_r \varepsilon_0} \qquad (4)$$

which we calculate to be 1.89 V/Å, and would correspond to a potential energy drop of ~ 80 V. When we inspect the field in BTO from the calculation, we see that the field is actually only 0.02 V/Å, roughly 1% of the field that we obtained under these assumptions. The reason for this discrepancy in field and potential difference will be discussed in the next section.

IV. Two-Dimensional Electron and Hole Gases

Further insight can be obtained from the analysis of the electronic structure of our heterostructures. We plot the layer projected density of states (DOS) of the TiO_2 layers in Figure 4. In Figure 4a we present the result for configuration P_0. For the surface TiO_2 layer, the DOS extends into the gap, due to the higher energy surface states at the TiO_2-terminated surface.[70] The rest of the TiO_2 layers are similar to that of bulk BTO. Also note that there is no large change in

the DOS at the BTO/STO interface, and the entire heterostructure is insulating. In the non-polarized case, there is no fundamental difference between this heterostructure and a relatively thick BTO or STO slab. The BaO-terminated case looks essentially the same as the P_0 case.

When examining the P_+ configuration (Figure 4b), however, there are important differences. First, there is the previously mentioned electric field across the BTO layer, which is expected for a polarized slab of BTO. More importantly, examining the STO/BTO interface, we see that the Fermi energy is now in the conduction band, indicating that the interface is conducting. Moving towards vacuum, away from the interface, the conduction band rises due to the internal field of BTO, and the Fermi energy drops below the conduction band edge, showing that the bulk of BTO is insulating. Finally, reaching the surface of BTO, we see that the Fermi energy is now in the valence band, making the surface also conducting. In Figure 4c we show the DOS for a range of energies closer to the Fermi energy. There is charge density near the interface that does not extend into the BTO bulk. This suggests that this conducting interfacial state has two-dimensional character, i.e. a 2DEG. Also, as the Fermi energy is in the surface layer of BTO, there is also a two-dimensional hole gas (2DHG) at the surface. Figure 5 shows a contour plot of the DOS that shows the 2DEG and 2DHG. As we can see, since neither of the materials are polar, there must be hole states present somewhere in the material, since the paraelectric heterostructure is charge neutral and insulating.

In Figure 6, we examine the projected DOS at the surface, interface, and deep in the STO bulk. We see that the 2DHG at the surface of BTO resides entirely on oxygen p_x and p_y states. The effect of the surface is to raise the energies of the p_x and p_y states while leaving the p_z states unaffected, consistent with prior calculations of the BTO surface.[72] The Ti d-states do not strongly contribute to this surface state. At both the BTO/STO interface and in the STO bulk, we see that the 2DEG is comprised of mostly Ti d_{yz} and d_{xz} states, with a small portion of d_{xy} states; the e_g states and O p-states do not contribute. This is quite different from the LAO/STO interface, where only the d_{xy} orbital is occupied, and forms an in-gap state.[12]

The difference in occupation is due to the symmetry-breaking nature of the interface, and the rumpling of the TiO_2 planes in STO, though the splitting of the t_{2g} states is small (this splitting is also seen in the nonpolarized heterostructure, although the t_{2g} states are unoccupied).

The charge density at the Fermi level of the heterostructure is shown in Figure 7. In Figure 7a, we see that the holes are localized completely at the BTO surface, on the O atoms (if exposed to air, this 2DHG might be compensated by adsorbed species, therefore in practice one may need to consider a capping layer). The p character of the charge density is clearly visible. In Figure 7b, we see that the electron density is located over several layers of TiO_2, concentrated at the interface, and dying rapidly into STO and BTO; it is located almost entirely on the Ti atoms**,** in agreement with our analysis from the density of states. As the hole states are localized solely at

the BTO surface, and the electron states are mainly at the STO/BTO interface, decaying rapidly going into both STO and BTO, we call these states two-dimensional.

One important issue is that, in LDA, both BTO and STO have an incorrect band gap (in experiment the band gap is ~3.2 eV for both rather than ~1.7 eV in LDA). Our calculations show that using the LDA+U[73] method in bulk BTO, with U on the Ti *d* states, bulk BTO is paraelectric, even in the tetragonal phase. This means that using relaxing the ions using LDA+U in the system is not possible, as we will be unable to achieve a ferroelectric state. However, we did a calculation with relaxed ionic positions with LDA, and we used LDA+U (U = 8.0 eV) to see its effect on the electronic structure. With LDA+U on bulk BTO, the gap is increased to ~2.8 eV, and upon examining the DOS for the polarized heterostructure, the 2DEG dies much more rapidly than in LDA, with the central layer of TiO_2 almost insulating (the paraelectric BTO/STO structure is essentially unchanged, except for the larger band gaps). This is to be expected, due to the scaling of shorter decay length with larger band gaps.[74]

Now, we discuss why the electric field in BTO is smaller than anticipated. The effect of the 2DHG and 2DEG is to impose an extra electric field on the BTO to help screen the large field caused by the polarization of the sample (here we assume that the field caused by the 2D gases almost entirely compensates the internal field caused by the polarization, see Figure 8). The electric field caused by the 2DHG and 2DEG points in the opposite direction to that of the field due to the polarization of BTO. We calculate the charge of the 2DHG by integrating the DOS for the surface layer of TiO_2 and find the total charge to be 0.12 e; the charge of the 2DEG must be opposite in value due to the conservation of charge in the system. We calculate the surface charge density of each gas to be 12.5 $\mu C/cm^2$. Therefore, the true electric field of the system is given by the difference between the two polarizations, which is 0.45 V/Å. Finally, we expect the field to be diminished in BTO due to its large dielectric constant. If we take the expected field and divide it by the calculated field, we obtain a relative dielectric constant of 21.0. Although this number is small in comparison to that of bulk BTO (1500 at 1 KHz),[75] experiment has shown that thin films have a much smaller relative dielectric constant (as low as 93 for 108 nm film).[76] As our film is even thinner (~ 4 nm), we believe that a value of 21.0 is a reasonable estimate for the dielectric constant of our sample.

There is another way to view the formation of the two-dimensional gases in our system. Electrostatic boundary conditions tell us that the free surface charge density σ_f of an interface is due to the difference in the normal component of the electric displacement **D** between two materials:

$$D_{1,n} - D_{2,n} = \sigma_f \qquad (5)$$

As there is no external field, we see that σ_f is due to the difference in polarization between BTO and STO. We compute the average polarization in STO to be 2.0 $\mu C/cm^2$, and thus σ_f is equal to 14.4 $\mu C/cm^2$, in good agreement with 12.5 $\mu C/cm^2$ of the 2DEG and 2DHG found from the integrated charge density (we can see that since the polarization is not constant in BTO and STO,

we do not expect this approximation to be exact). Thus, we see that the presence of the gases can also be explained with an electrostatic argument.

The mechanism for the formation of the conducting layers is similar to that at the LAO/STO interface. The internal field due to the polarization in BTO increases with increasing BTO thickness. There is an electronic reconstruction caused by the migration of the electrons in the high-energy surface state to the BTO/STO interface to avoid the polar catastrophe, similarly to that at the LAO/STO interface. In our calculation, however, the 2DEG is comprised of all t_{2g} states, in contrast with the LAO/STO interface that has a 2DEG only in the d_{xy} orbital. In addition, while in LAO there is no mechanism to "turn-off" the field due to the intrinsically polar layers, in BTO the field can be removed by switching to a non-polar state, where the TiO_2 layers are flat and there is no field. In this case, there is no polar catastrophe and the electronic reconstruction is unnecessary, leading to an insulating interface, which is to be expected for a clean interface between two non-polar oxides. This gives us control over having a conducting or insulating interface and surface by switching between two stable polarization states. A possible way to check this experimentally would be to measure interface conductivity of a BTO/STO heterostructure above and below the critical temperature T_c of BTO.

V. Conclusion

Using first-principles calculations, we investigate the interface between a ferroelectric BTO film and a non-polar insulating STO substrate. We find that thin TiO_2-terminated BTO, under 5 nm, can stabilize two different polarization states; one is a paraelectric state, and the other is a polarized state where BTO is polarized toward the BTO/STO interface. There is a potential difference of 0.81 eV in STO between the non-polarized and the polarized BTO heterostructures caused by the drop in potential from the electric field created by the BTO polarization. The non-polarized heterostructure is insulating throughout and no two-dimensional conductive states are found. In the polarized heterostructure; however, we discovered the existence of a 2DEG at the interface between BTO and STO, and the existence of a 2DHG at the surface of BTO. The polarized heterostructure undergoes an electronic reconstruction in order prevent the polar catastrophe, which explains the appearance of both the 2DEG and 2DHG. The two-dimensional gases cause an additional electric field in BTO that opposes the field caused by the polarization, leading to a substantially reduced potential drop. We calculate the relative dielectric constant of the thin BTO film to be 21.0. We emphasize that the creation of this 2DEG at an insulating oxide interface has been shown to be created by the polarization of the sample, and not due to polar materials or doping.

Acknowledgements

We are grateful to Chungwei Lin and Agham Posadas for critical reading of the manuscript and constructive suggestions. This work was supported by the National Science Foundation (Award DMR-1207342), the Air Force Office of Scientific Research (Grant FA9550–12–10494), and Texas Advanced Computing Center.

Figure Captions

Figure 1. The simulation cell, showing the Vacuum/BTO/STO/BTO/Vacuum slab.

Figure 2. The a) rumpling and b) polarization for the paraelectric P_0 structure, and the c) rumpling and d) polarization for the polarized P_+ structure.

Figure 3. The comparison of plane-averaged electron electrostatic potential between P_0 and P_+. The difference in potential due to the polarization in the P_+ case can be clearly seen.

Figure 4. The layer-decomposed DOS for a) P0 and b) P+. The slab is mirrored on the other side, so only a half of the DOS is shown.

Figure 5. The DOS of the system projected on TiO_2 planes in the energy vs distance plane for the a) polarized and b) paraelectric BTO/STO heterostructure. In the polarized case, the 2DEG and the 2DHG can be clearly seen.

Figure 6. Projected DOS for selected TiO2 planes for the polarized BTO/STO heterostructure. a) p-states and b) d-states of the BTO surface, c) p-states and d) d-states of the BTO/STO interface, and e) p-states and f) d-states of the center of the STO bulk. The 2DEG can be seen to be of almost all d-character, and the 2DHG can be seen to be almost entirely p-character.

Figure 7. The charge density at the Fermi level. The pictured isosurface is for a charge density of 0.1203 $e/Å^3$. a) The hole gas at the surface of BTO. Note the p-character of the charge density. b) The electron gas at the STO/BTO interface. Note the d-character of the charge distribution.

Figure 8. a) The electric field caused by the polarization of BTO. b) The electric field caused by the 2DEG and 2DHG. Note that the gases cause a field that opposes the field caused by the polarization of the sample.

References

[1] A. Ohtomo and H.Y. Hwang, Nature **427**, 423 (2004).

[2] J. Goniakowski, F. Finocchi, and C. Noguera, Reports Prog. Phys. **71**, 016501 (2008).

[3] H.Y. Hwang, Science **313**, 1895 (2006).

[4] W. Harrison, E. Kraut, J. Waldrop, and R. Grant, Phys. Rev. B **18**, 4402 (1978).

[5] N. Nakagawa, H.Y. Hwang, and D. a. Muller, Nat. Mater. **5**, 204 (2006).

[6] A. Kalabukhov, R. Gunnarsson, J. Börjesson, E. Olsson, T. Claeson, and D. Winkler, Phys. Rev. B **75**, 121404 (2007).

[7] W. Siemons, G. Koster, H. Yamamoto, W. Harrison, G. Lucovsky, T. Geballe, D. Blank, and M. Beasley, Phys. Rev. Lett. **98**, 196802 (2007).

[8] H.Y. Hwang, Y. Iwasa, M. Kawasaki, B. Keimer, N. Nagaosa, and Y. Tokura, Nat. Mater. **11**, 103 (2012).

[9] G. Herranz, M. Basletić, M. Bibes, C. Carrétéro, E. Tafra, E. Jacquet, K. Bouzehouane, C. Deranlot, A. Hamzić, J.-M. Broto, A. Barthélémy, and A. Fert, Phys. Rev. Lett. **98**, 216803 (2007).

[10] H. Seo and A.A. Demkov, Phys. Rev. B **84**, 045440 (2011).

[11] R. Pentcheva and W. Pickett, Phys. Rev. B **74**, 035112 (2006).

[12] J. Lee and A.A. Demkov, Phys. Rev. B **78**, 193104 (2008).

[13] K. Janicka, J. Velev, and E. Tsymbal, Phys. Rev. Lett. **102**, 106803 (2009).

[14] S. Thiel, G. Hammerl, A. Schmehl, C.W. Schneider, and J. Mannhart, Science **313**, 1942 (2006).

[15] M. Huijben, G. Rijnders, D.H.A. Blank, S. Bals, S. Van Aert, J. Verbeeck, G. Van Tendeloo, A. Brinkman, and H. Hilgenkamp, Nat. Mater. **5**, 556 (2006).

[16] Z. Popović, S. Satpathy, and R. Martin, Phys. Rev. Lett. **101**, 256801 (2008).

[17] A. Brinkman, M. Huijben, M. van Zalk, J. Huijben, U. Zeitler, J.C. Maan, W.G. van der Wiel, G. Rijnders, D.H.A. Blank, and H. Hilgenkamp, Nat. Mater. **6**, 493 (2007).

[18] C.W. Bark, D.A. Felker, Y. Wang, Y. Zhang, H.W. Jang, C.M. Folkman, J.W. Park, S.H. Baek, H. Zhou, D.D. Fong, X.Q. Pan, E.Y. Tsymbal, M.S. Rzchowski, and C.B. Eom, Proc. Natl. Acad. Sci. **108**, 4720 (2011).

[19] N. Reyren, S. Thiel, A.D. Caviglia, L.F. Kourkoutis, G. Hammerl, C. Richter, C.W. Schneider, T. Kopp, A.-S. Rüetschi, D. Jaccard, M. Gabay, D.A. Muller, J.-M. Triscone, and J. Mannhart, Science **317**, 1196 (2007).

[20] A.D. Caviglia, S. Gariglio, N. Reyren, D. Jaccard, T. Schneider, M. Gabay, S. Thiel, G. Hammerl, J. Mannhart, and J.-M. Triscone, Nature **456**, 624 (2008).

[21] A. Manchon and S. Zhang, Phys. Rev. B **78**, 212405 (2008).

[22] G. Khalsa, B. Lee, and A.H. MacDonald, Phys. Rev. B **88**, 041302 (2013).

[23] a. D. Caviglia, M. Gabay, S. Gariglio, N. Reyren, C. Cancellieri, and J.-M. Triscone, Phys. Rev. Lett. **104**, 126803 (2010).

[24] M. Basletic, J.-L. Maurice, C. Carrétéro, G. Herranz, O. Copie, M. Bibes, E. Jacquet, K. Bouzehouane, S. Fusil, and A. Barthélémy, Nat. Mater. **7**, 621 (2008).

[25] G. Khalsa and A.H. MacDonald, Phys. Rev. B **86**, 125121 (2012).

[26] M. Takizawa, H. Wadati, K. Tanaka, M. Hashimoto, T. Yoshida, A. Fujimori, A. Chikamatsu, H. Kumigashira, M. Oshima, K. Shibuya, T. Mihara, T. Ohnishi, M. Lippmaa, M. Kawasaki, H. Koinuma, S. Okamoto, and A. Millis, Phys. Rev. Lett. **97**, 057601 (2006).

[27] S. Okamoto, A. Millis, and N. Spaldin, Phys. Rev. Lett. **97**, 056802 (2006).

[28] A. Ohtomo, D.A. Muller, J.L. Grazul, and H.Y. Hwang, Nature **419**, 378 (2002).

[29] R. Pentcheva and W. Pickett, Phys. Rev. Lett. **102**, 107602 (2009).

[30] R. Arras, V.G. Ruiz, W.E. Pickett, and R. Pentcheva, Phys. Rev. B **85**, 125404 (2012).

[31] J.W. Park, D.F. Bogorin, C. Cen, D.A. Felker, Y. Zhang, C.T. Nelson, C.W. Bark, C.M. Folkman, X.Q. Pan, M.S. Rzchowski, J. Levy, and C.B. Eom, Nat. Commun. **1**, 94 (2010).

[32] C. Cen, S. Thiel, J. Mannhart, and J. Levy, Science **323**, 1026 (2009).

[33] C. Cen, S. Thiel, G. Hammerl, C.W. Schneider, K.E. Andersen, C.S. Hellberg, J. Mannhart, and J. Levy, Nat. Mater. **7**, 298 (2008).

[34] H.W. Jang, D. a Felker, C.W. Bark, Y. Wang, M.K. Niranjan, C.T. Nelson, Y. Zhang, D. Su, C.M. Folkman, S.H. Baek, S. Lee, K. Janicka, Y. Zhu, X.Q. Pan, D.D. Fong, E.Y. Tsymbal, M.S. Rzchowski, and C.B. Eom, Science **331**, 886 (2011).

[35] P. V. Ong, J. Lee, and W.E. Pickett, Phys. Rev. B **83**, 193106 (2011).

[36] N. Sai, J. Lee, C.J. Fennie, and A. a. Demkov, Appl. Phys. Lett. **91**, 202910 (2007).

[37] Y. Kozuka, A. Tsukazaki, and M. Kawasaki, Appl. Phys. Rev. **1**, 011303 (2014).

[38] P. Anderson and E. Blount, **14**, 217 (1965).

[39] T. Kolodiazhnyi, M. Tachibana, H. Kawaji, J. Hwang, and E. Takayama-Muromachi, Phys. Rev. Lett. **104**, 147602 (2010).

[40] Y. Wang, X. Liu, J.D. Burton, S.S. Jaswal, and E.Y. Tsymbal, Phys. Rev. Lett. **109**, 247601 (2012).

[41] Y. Shi, Y. Guo, X. Wang, A.J. Princep, D. Khalyavin, P. Manuel, Y. Michiue, A. Sato, K. Tsuda, S. Yu, M. Arai, Y. Shirako, M. Akaogi, N. Wang, K. Yamaura, and A.T. Boothroyd, Nat. Mater. **12**, 1024 (2013).

[42] J. He, G.B. Stephenson, and S.M. Nakhmanson, J. Appl. Phys. **112**, 054112 (2012).

[43] Y. Watanabe, M. Okano, and A. Masuda, Phys. Rev. Lett. **86**, 332 (2001).

[44] M.S.J. Marshall, A. Malashevich, A.S. Disa, M.-G. Han, H. Chen, Y. Zhu, S. Ismail-Beigi, F.J. Walker, and C.H. Ahn, Phys. Rev. Appl. **2**, 051001 (2014).

[45] M. Niranjan, Y. Wang, S. Jaswal, and E. Tsymbal, Phys. Rev. Lett. **103**, 016804 (2009).

[46] K. Shimoyama, M. Kiyohara, K. Kubo, A. Uedono, and K. Yamabe, J. Appl. Phys. **92**, 4625 (2002).

[47] A. Soukiassian, W. Tian, V. Vaithyanathan, J.H. Haeni, L.Q. Chen, X.X. Xi, D.G. Schlom, D. a. Tenne, H.P. Sun, X.Q. Pan, K.J. Choi, C.B. Eom, Y.L. Li, Q.X. Jia, C. Constantin, R.M. Feenstra, M. Bernhagen, P. Reiche, and R. Uecker, J. Mater. Res. **23**, 1417 (2011).

[48] A. Visinoiu, R. Scholz, S. Chattopadhyay, M. Alexe, and D. Hesse, Jpn. J. Appl. Phys. **41**, 6633 (2002).

[49] J.B. Neaton and K.M. Rabe, Appl. Phys. Lett. **82**, 1586 (2003).

[50] a. L. Roytburd, S. Zhong, and S.P. Alpay, Appl. Phys. Lett. **87**, 1 (2005).

[51] G. Kresse and J. Furthmüller, Comput. Mater. Sci. **6**, 15 (1996).

[52] G. Kresse and J. Furthmüller, Phys. Rev. B **54**, 11169 (1996).

[53] G. Kresse and J. Hafner, Phys. Rev. B **47**, 558 (1993).

[54] G. Kresse and J. Hafner, Phys. Rev. B **49**, 14251 (1994).

[55] G. Kresse and D. Joubert, Phys. Rev. B **59**, 1758 (1999).

[56] P.E. Blöchl, Phys. Rev. B **50**, 17953 (1994).

[57] J. Perdew and A. Zunger, Phys. Rev. B **23**, 5048 (1981).

[58] H.J. Monkhorst and J.D. Pack, Phys. Rev. B **13**, 5188 (1976).

[59] E. Geiss, R. Sandstrom, W. Gallagher, A. Gupta, S. Shinde, R. Cook, E. Cooper, E. O'Sullivan, J. Roldan, A. Segmuller, and J. Angiello, IBM J. Res. Dev. **34**, 916 (1990).

[60] X. Zhang and A. a. Demkov, J. Vac. Sci. Technol. B Microelectron. Nanom. Struct. **20**, 1664 (2002).

[61] C. Li, D. Cui, Y. Zhou, H. Lu, and Z. Chen, Appl. Surf. Sci. **136**, 173 (1998).

[62] S. Tinte, M. Stachiotti, M. Sepliarsky, R. Migoni, and C. Rodriguez, J. Phys. Condens. Matter **11**, 9679 (1999).

[63] J. Junquera and P. Ghosez, Nature **422**, 506 (2003).

[64] M. Gajdoš, K. Hummer, G. Kresse, J. Furthmüller, and F. Bechstedt, Phys. Rev. B **73**, 045112 (2006).

[65] S. Baroni and R. Resta, Phys. Rev. B **33**, 7017 (1986).

[66] R. Resta, M. Posternak, and A. Baldereschi, Phys. Rev. Lett. **70**, 1010 (1993).

[67] W. Zhong, R. King-Smith, and D. Vanderbilt, Phys. Rev. Lett. **72**, 3618 (1994).

[68] H. Wieder, Phys. Rev. **1050**, 1161 (1955).

[69] R. Eglitis and D. Vanderbilt, Phys. Rev. B **76**, 155439 (2007).

[70] J. Padilla and D. Vanderbilt, Phys. Rev. B **418**, 64 (1997).

[71] K.D. Fredrickson, A.B. Posadas, A.A. Demkov, C. Dubourdieu, and J. Bruley, J. Appl. Phys. **113**, 184102 (2013).

[72] R.I. Eglitis, S. Piskunov, E. Heifets, E. a. Kotomin, and G. Borstel, Ceram. Int. **30**, 1989 (2004).

[73] S.L. Dudarev, G.A. Button, S.Y. Savrasov, C.J. Humphreys, and A.P. Sutton, Phys. Rev. B **57**, 1505 (1998).

[74] a. Demkov, L. Fonseca, E. Verret, J. Tomfohr, and O. Sankey, Phys. Rev. B **71**, 195306 (2005).

[75] B. Jaffe, W. Cook, and H. Jaffe, *Piezoelectric Ceramics* (Academic, New York, 1971).

[76] L. Huang, Z. Chen, J.D. Wilson, S. Banerjee, R.D. Robinson, I.P. Herman, R. Laibowitz, and S. O'Brien, J. Appl. Phys. **100**, 034316 (2006).

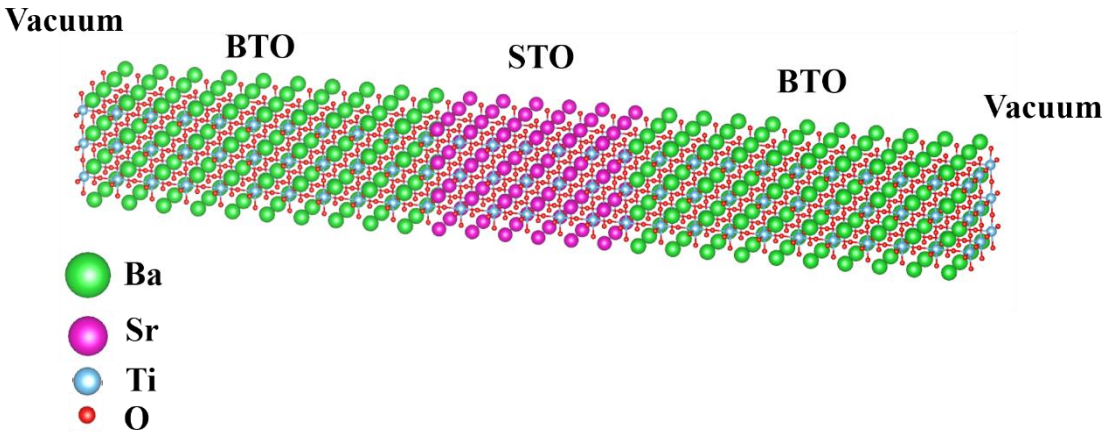
Vacuum
BTO
STO
BTO
Vacuum
Ba
Sr
Ti
O

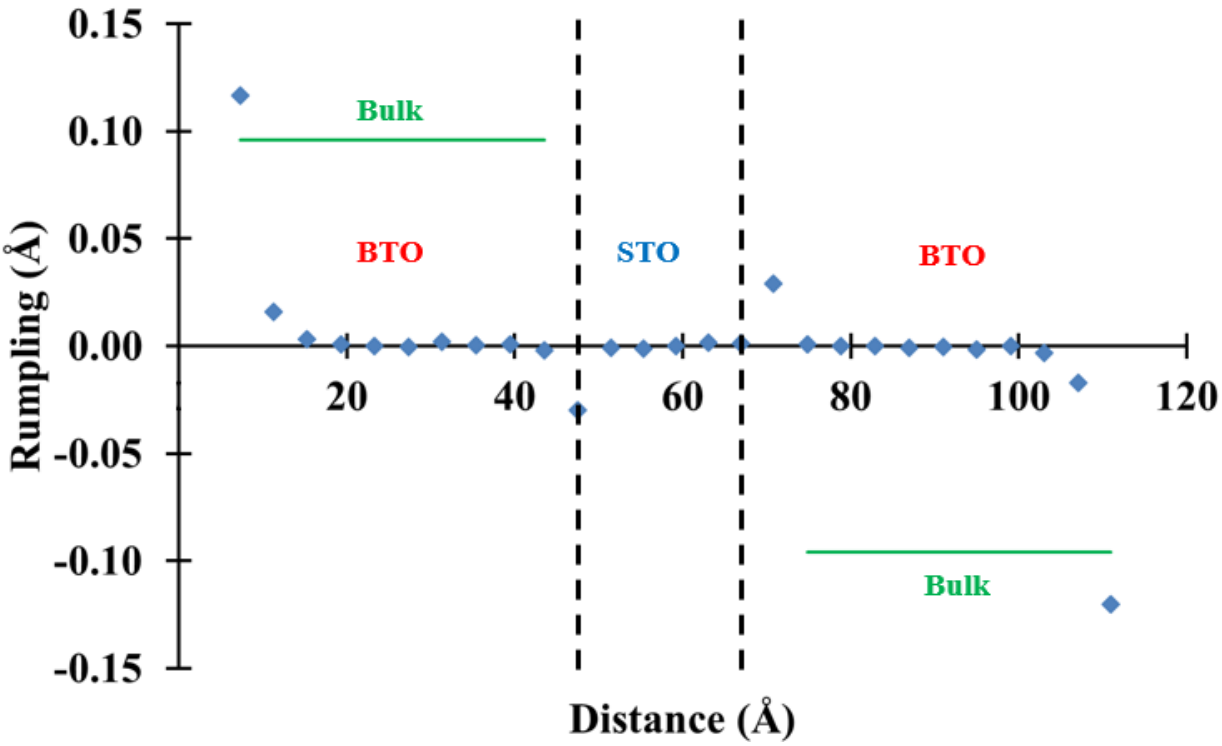
0.15
0.10
0.05
0.00
-0.05
-0.10
-0.15
Rumpling (Å)
20
40
60
80
100
120
Distance (Å)
Bulk
BTO
STO
BTO
Bulk

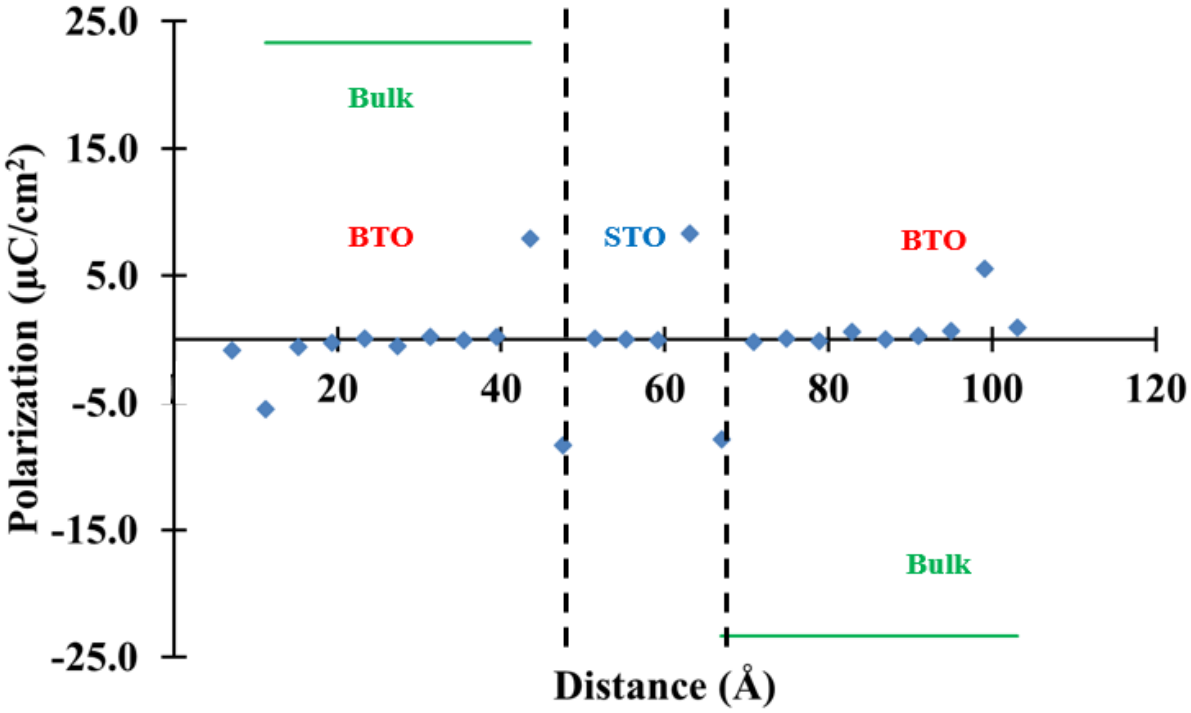
25.0
15.0
5.0
-5.0
-15.0
-25.0
Polarization (μC/cm²)
20
40
60
80
100
120
Distance (Å)
Bulk
BTO
STO
BTO
Bulk

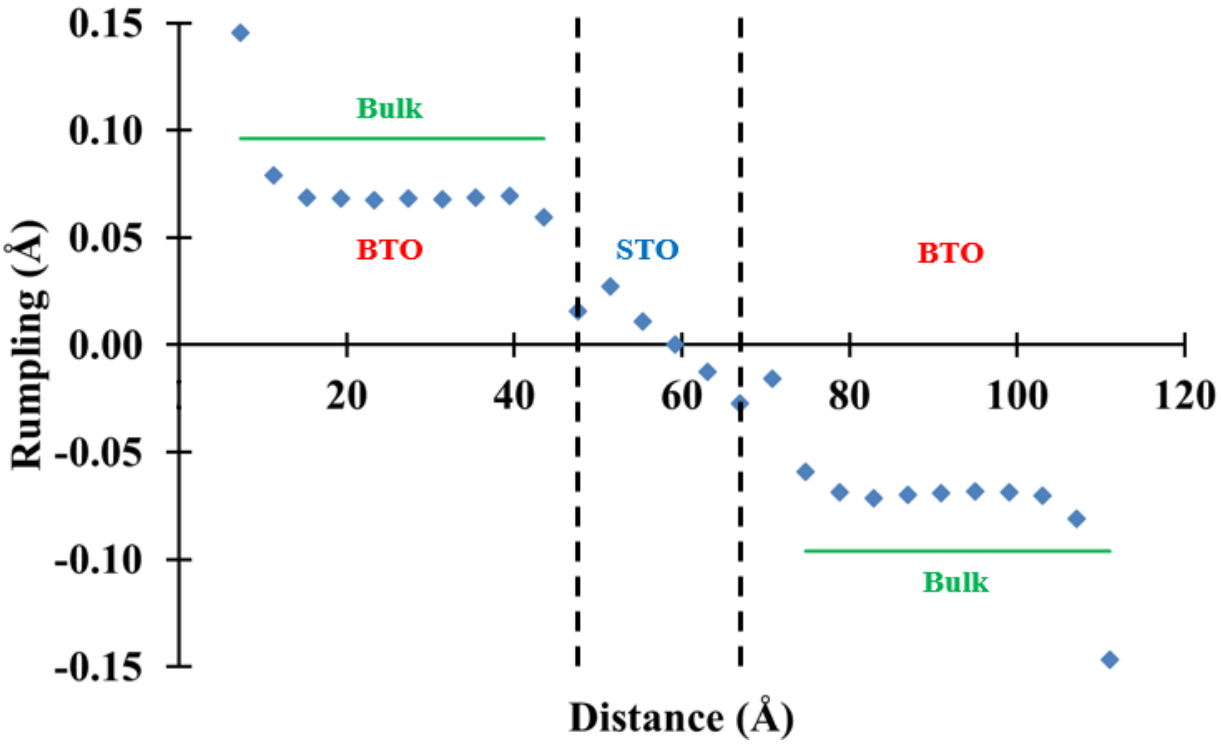
0.15
0.10
0.05
0.00
-0.05
-0.10
-0.15
Rumpling (Å)
20
40
60
80
100
120
Distance (Å)
Bulk
BTO
STO
BTO
Bulk

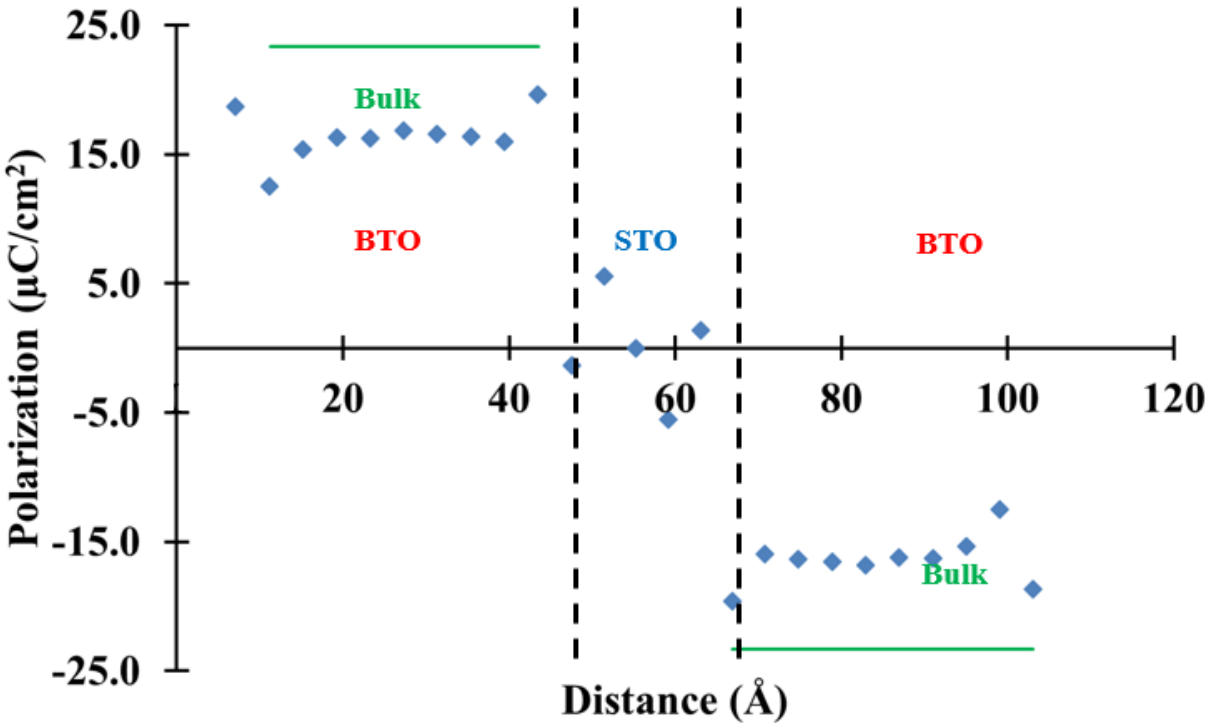
25.0
15.0
5.0
-5.0
-15.0
-25.0
Polarization (μC/cm²)
20
40
60
80
100
120
Distance (Å)
Bulk
BTO
STO
BTO
Bulk

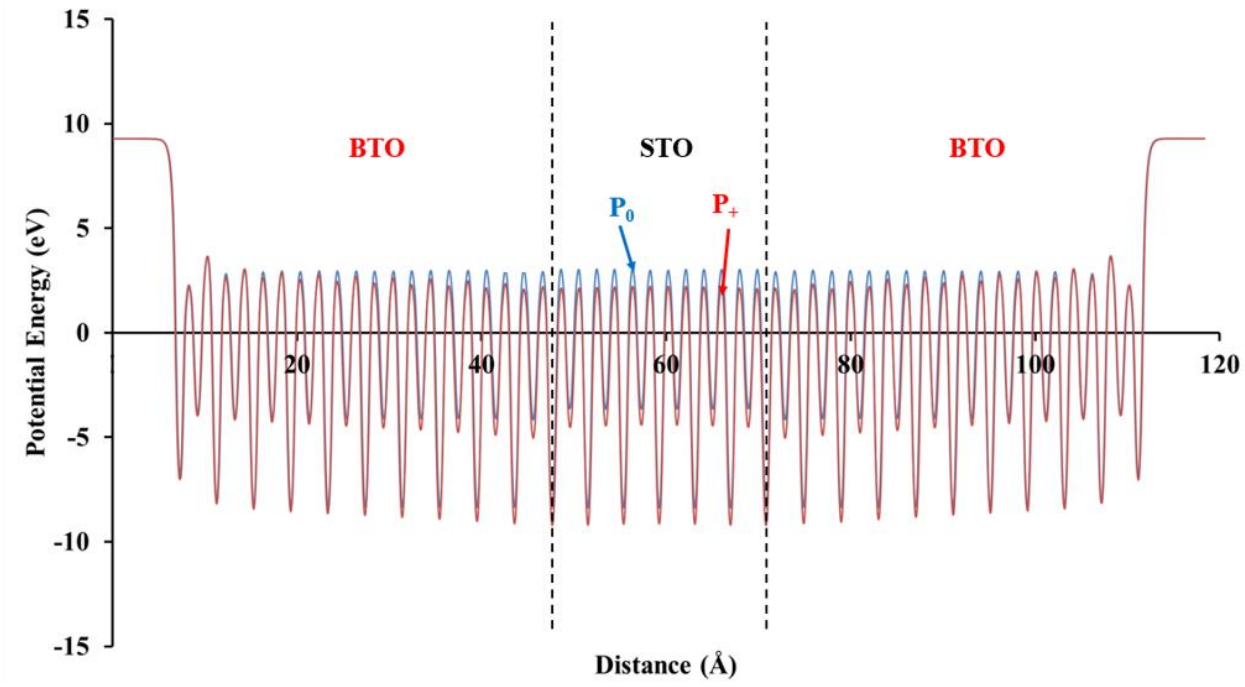
15
10
5
0
-5
-10
-15
Potential Energy (eV)
BTO
STO
BTO
P0
P+
20
40
60
80
100
120
Distance (Å)

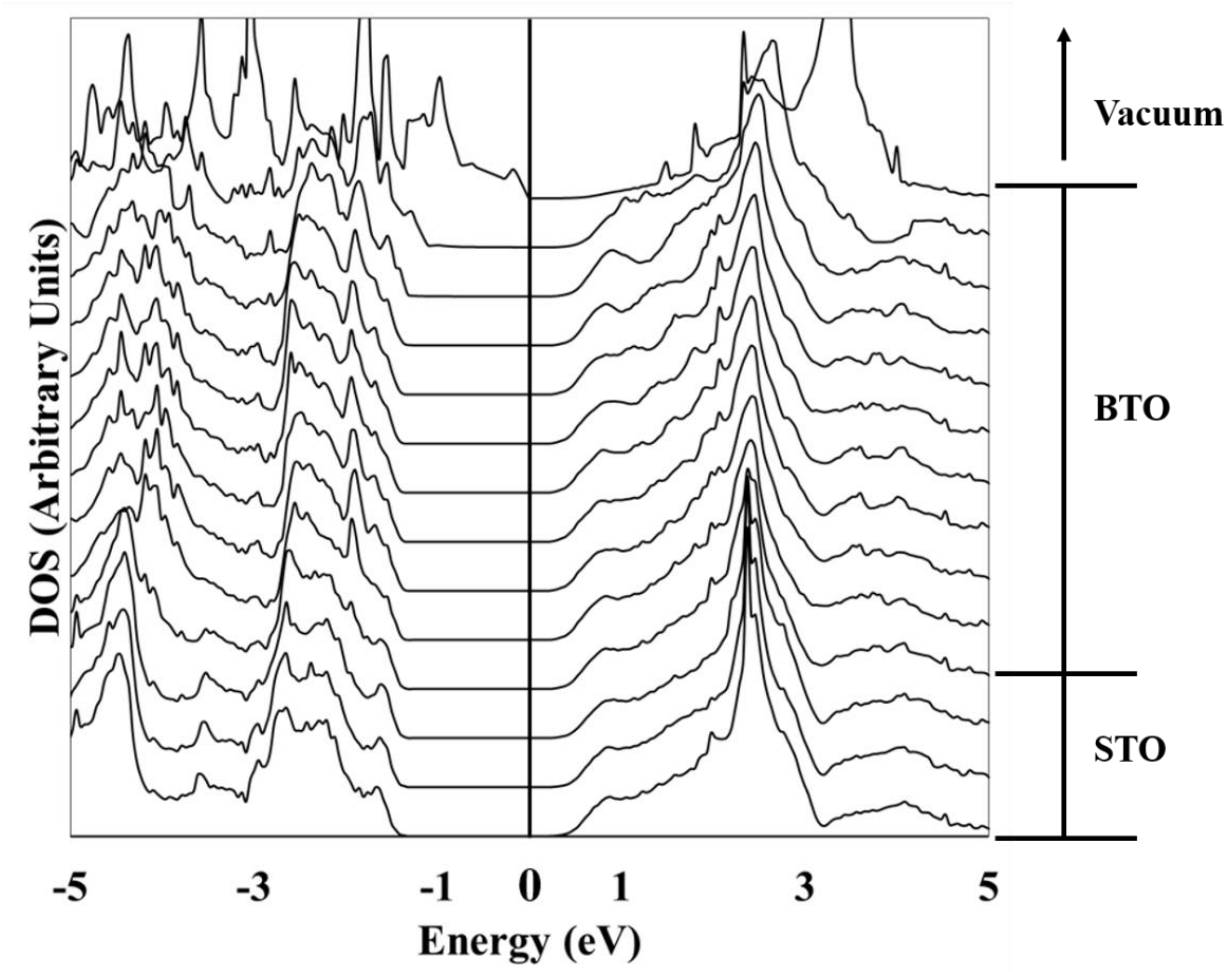
Vacuum
BTO
STO
DOS (Arbitrary Units)
-5
-3
-1
0
1
3
5
Energy (eV)

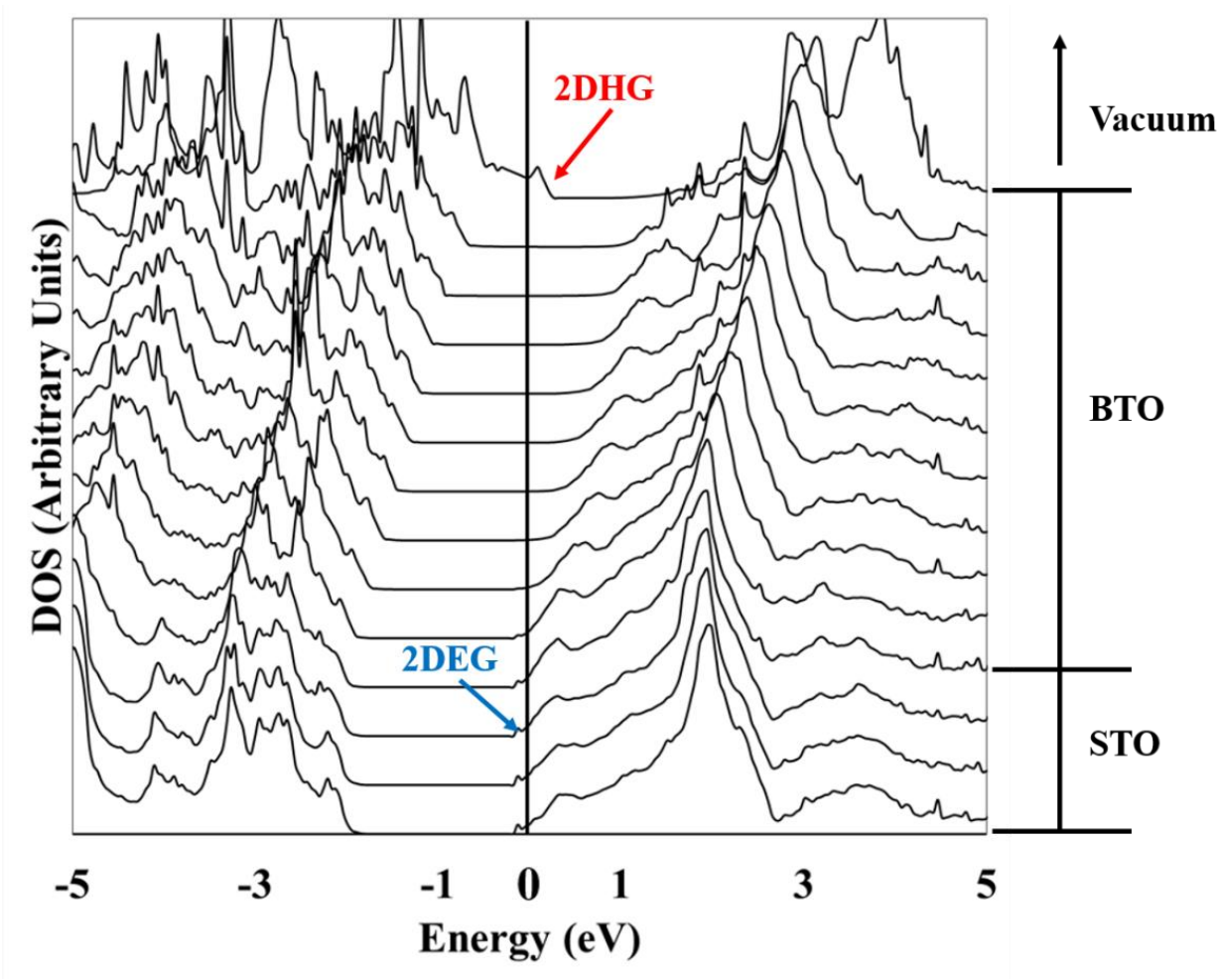
2DHG
2DEG
Vacuum
BTO
STO
DOS (Arbitrary Units)
-5
-3
-1
0
1
3
5
Energy (eV)

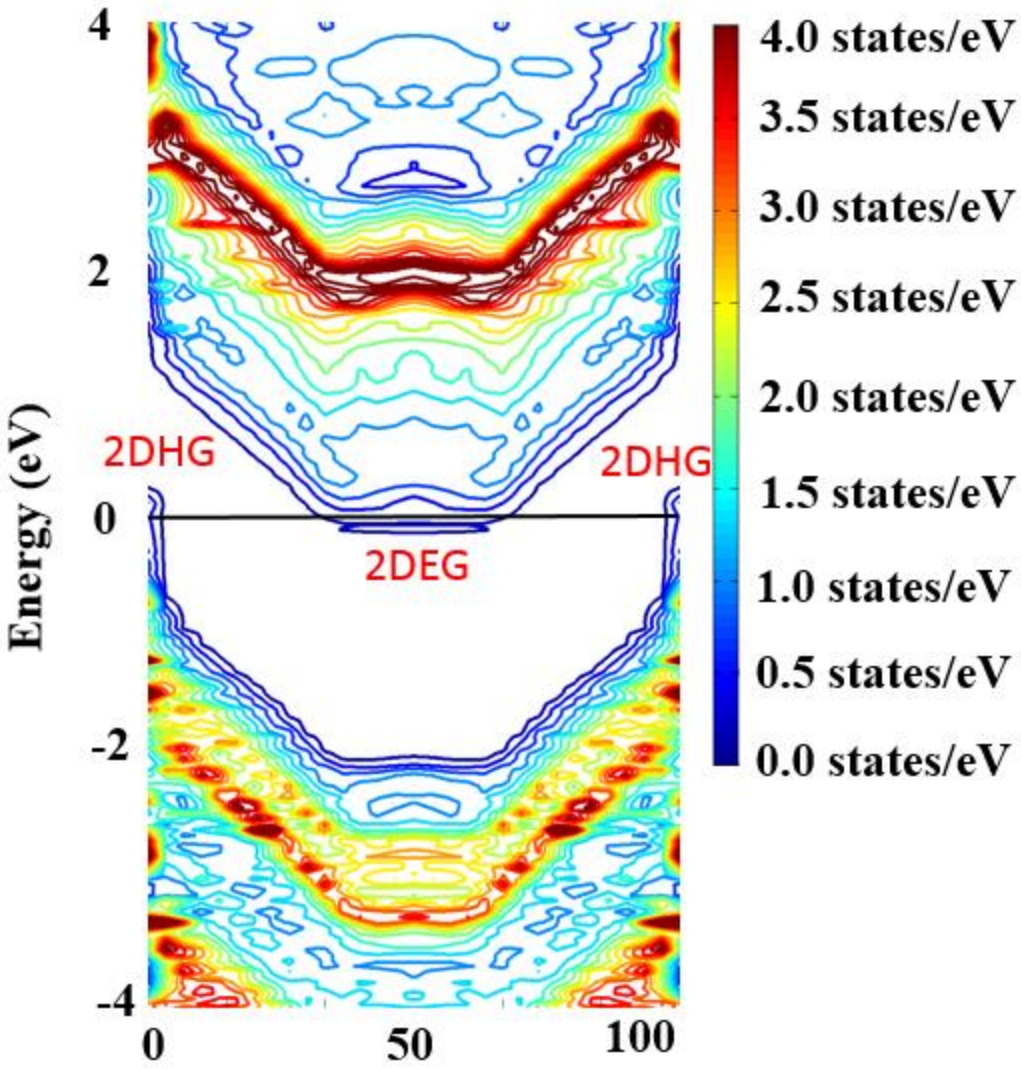
4
2
0
-2
-4
Energy (eV)
2DHG
2DHG
2DEG
0
50
100
4.0 states/eV
3.5 states/eV
3.0 states/eV
2.5 states/eV
2.0 states/eV
1.5 states/eV
1.0 states/eV
0.5 states/eV
0.0 states/eV

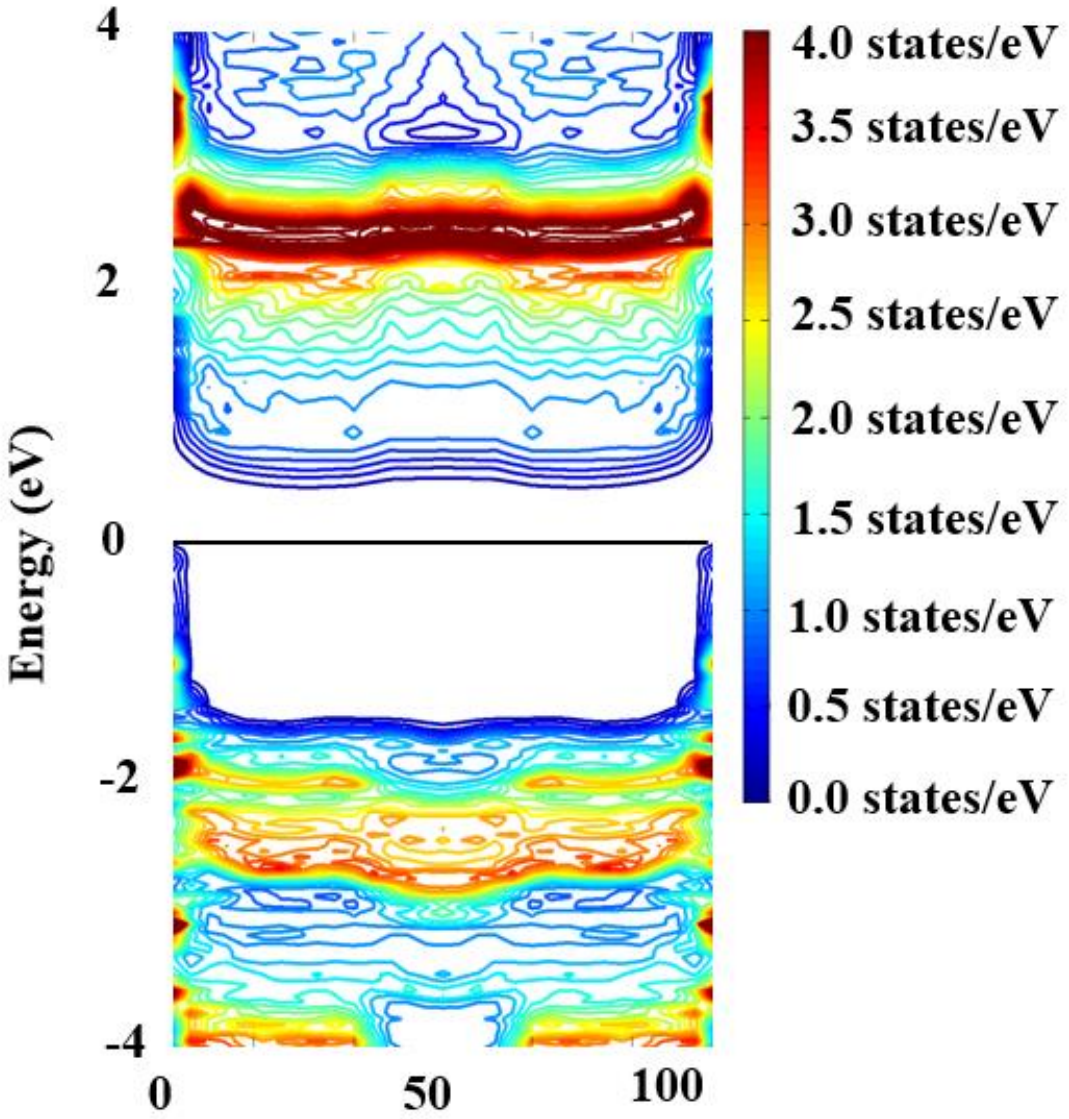
4
2
0
-2
-4
Energy (eV)
0
50
100
4.0 states/eV
3.5 states/eV
3.0 states/eV
2.5 states/eV
2.0 states/eV
1.5 states/eV
1.0 states/eV
0.5 states/eV
0.0 states/eV

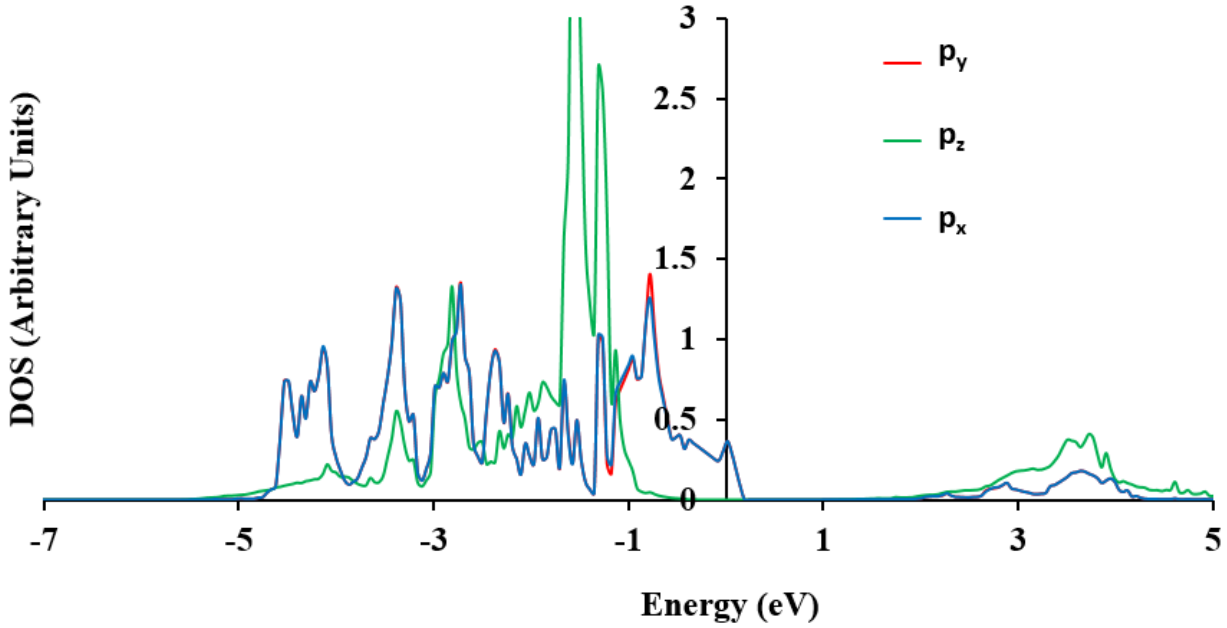
DOS (Arbitrary Units)
3
2.5
2
1.5
1
0.5
0
-7
-5
-3
-1
1
3
5
Energy (eV)
p_y
p_z
p_x

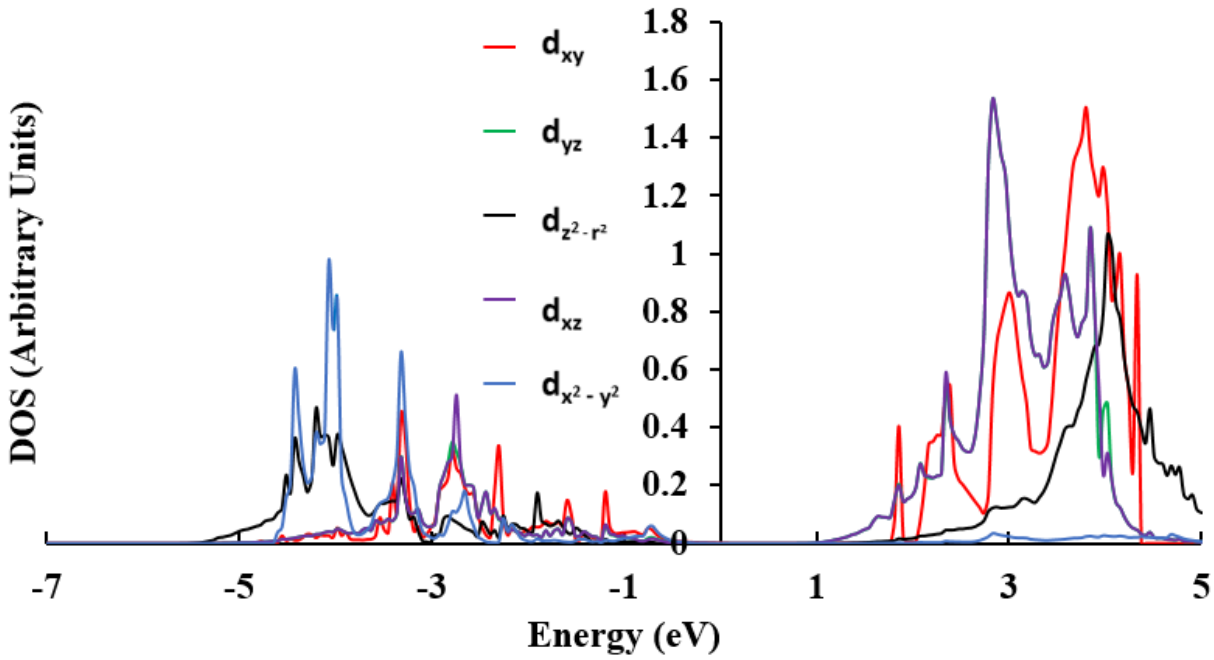
DOS (Arbitrary Units)
Energy (eV)
d_xy
d_yz
d_z² - r²
d_xz
d_x² - y²
1.8
1.6
1.4
1.2
1
0.8
0.6
0.4
0.2
0
-7
-5
-3
-1
1
3
5

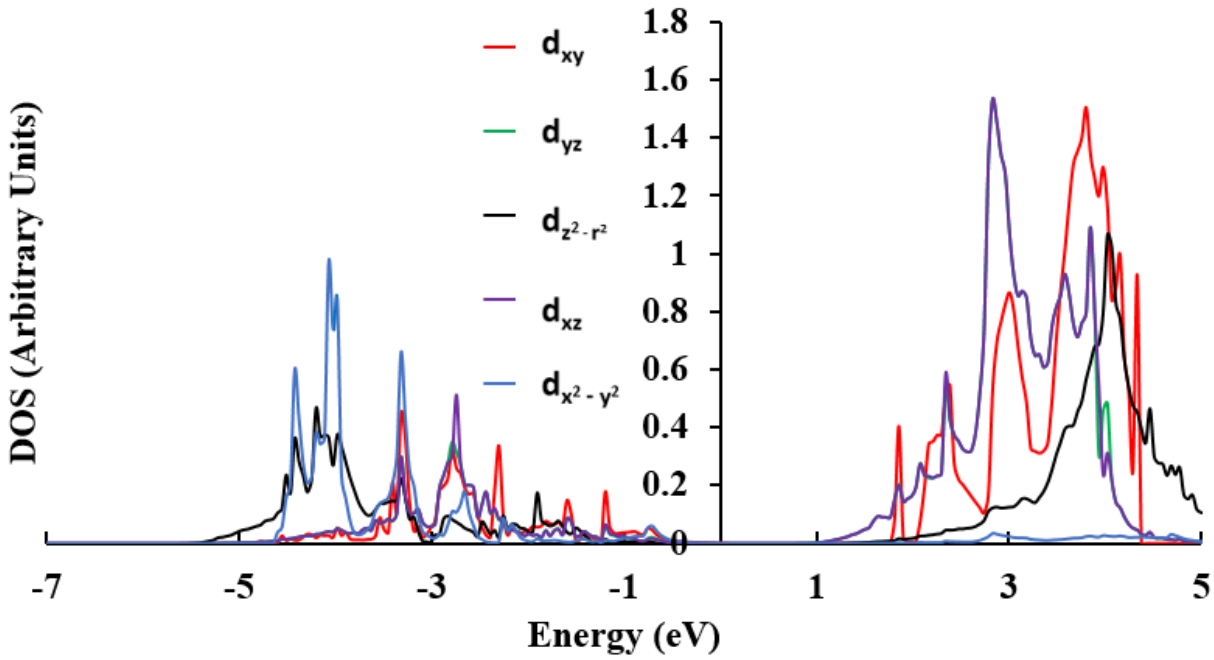
DOS (Arbitrary Units)
Energy (eV)
d_xy
d_yz
d_z² - r²
d_xz
d_x² - y²
1.8
1.6
1.4
1.2
1
0.8
0.6
0.4
0.2
0
-7
-5
-3
-1
1
3
5

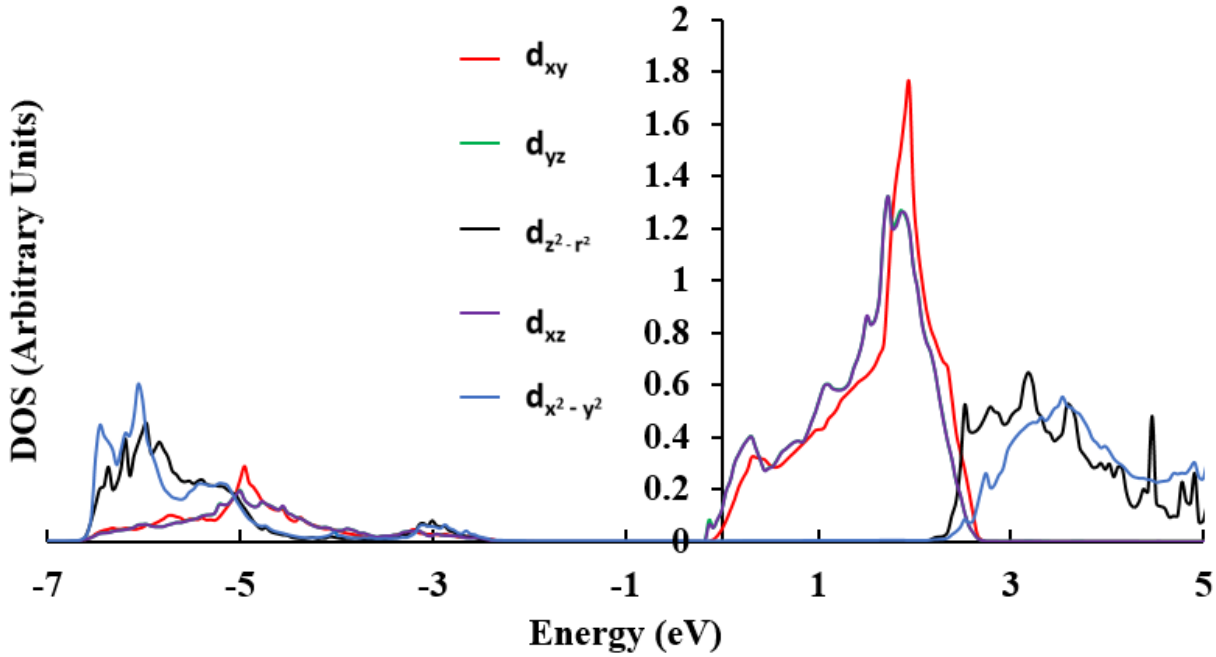
DOS (Arbitrary Units)
Energy (eV)
d_xy
d_yz
d_z²-r²
d_xz
d_x²-y²
2
1.8
1.6
1.4
1.2
1
0.8
0.6
0.4
0.2
0
-7
-5
-3
-1
1
3
5

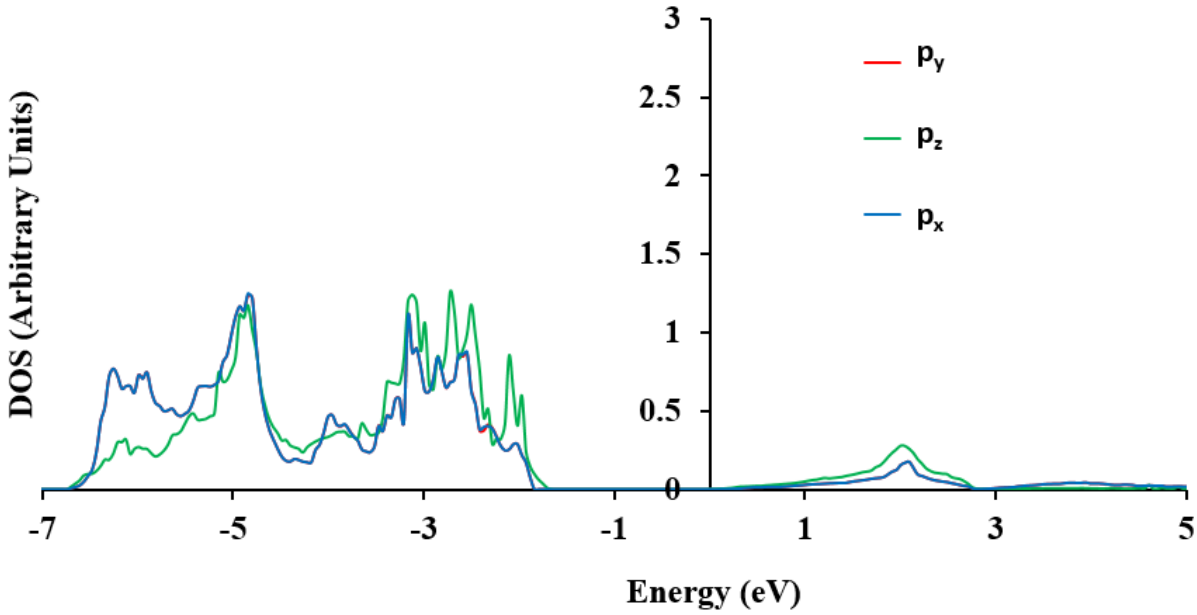
DOS (Arbitrary Units)
3
2.5
2
1.5
1
0.5
0
-7
-5
-3
-1
1
3
5
Energy (eV)
p_y
p_z
p_x

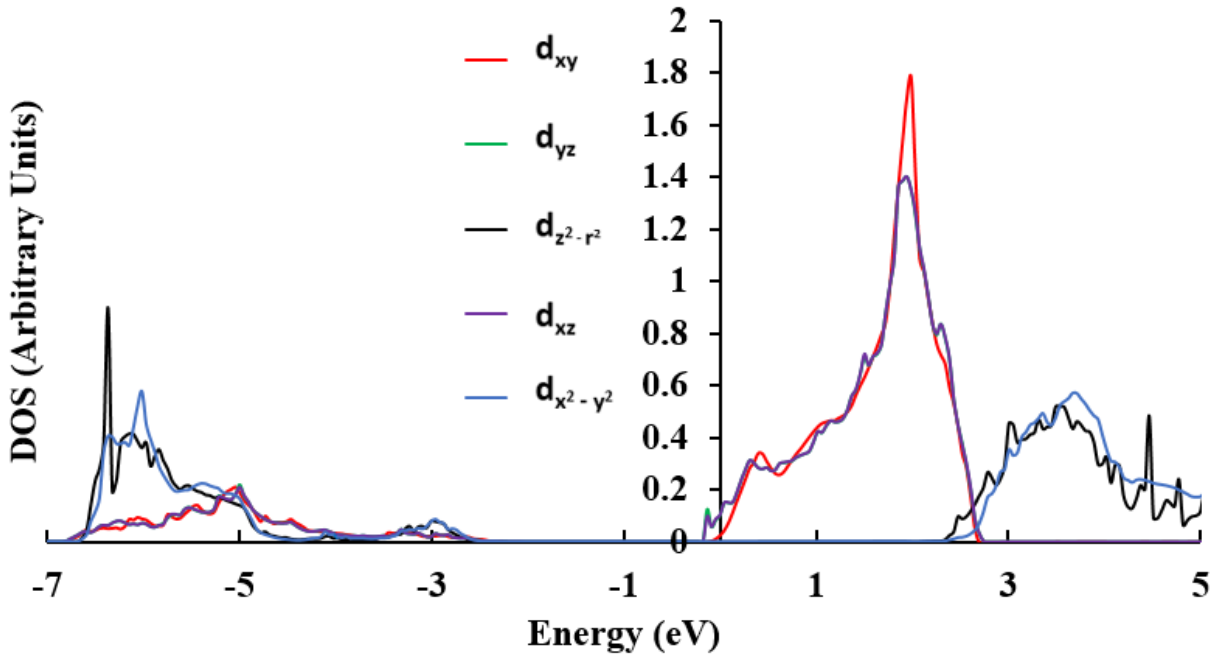
DOS (Arbitrary Units)
Energy (eV)
d_xy
d_yz
d_z²-r²
d_xz
d_x²-y²
2
1.8
1.6
1.4
1.2
1
0.8
0.6
0.4
0.2
0
-7
-5
-3
-1
1
3
5

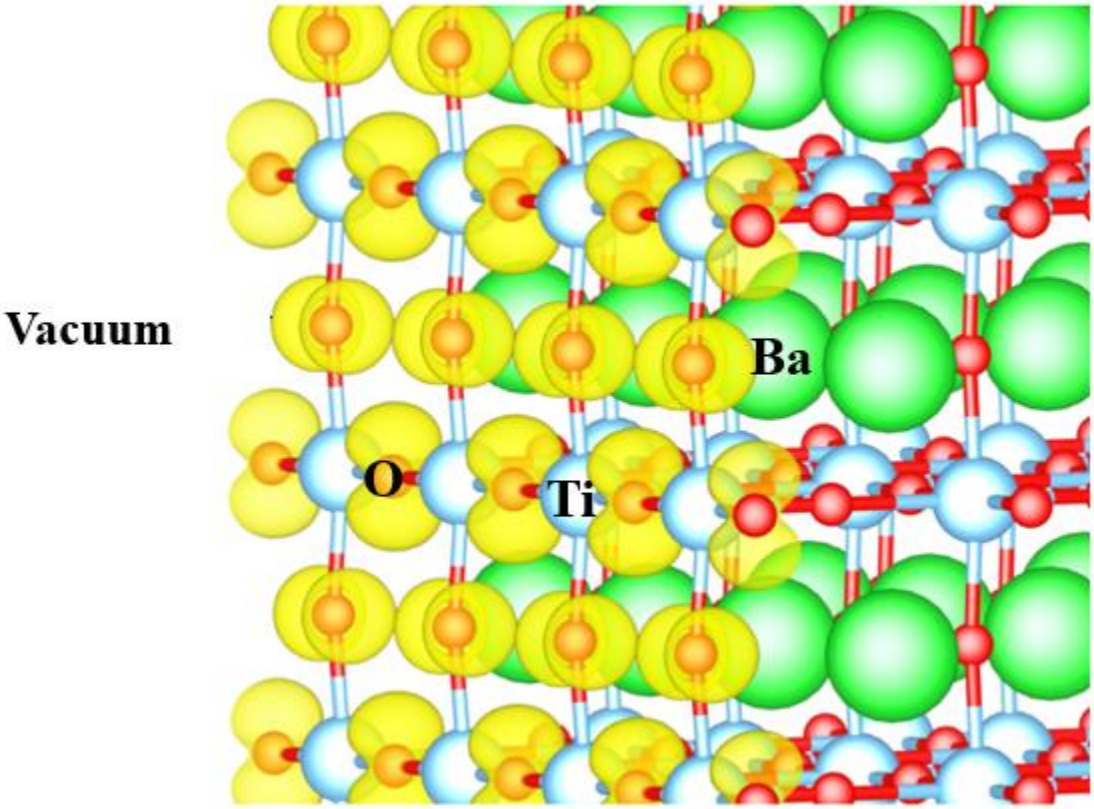
Vacuum
Ba
O
Ti

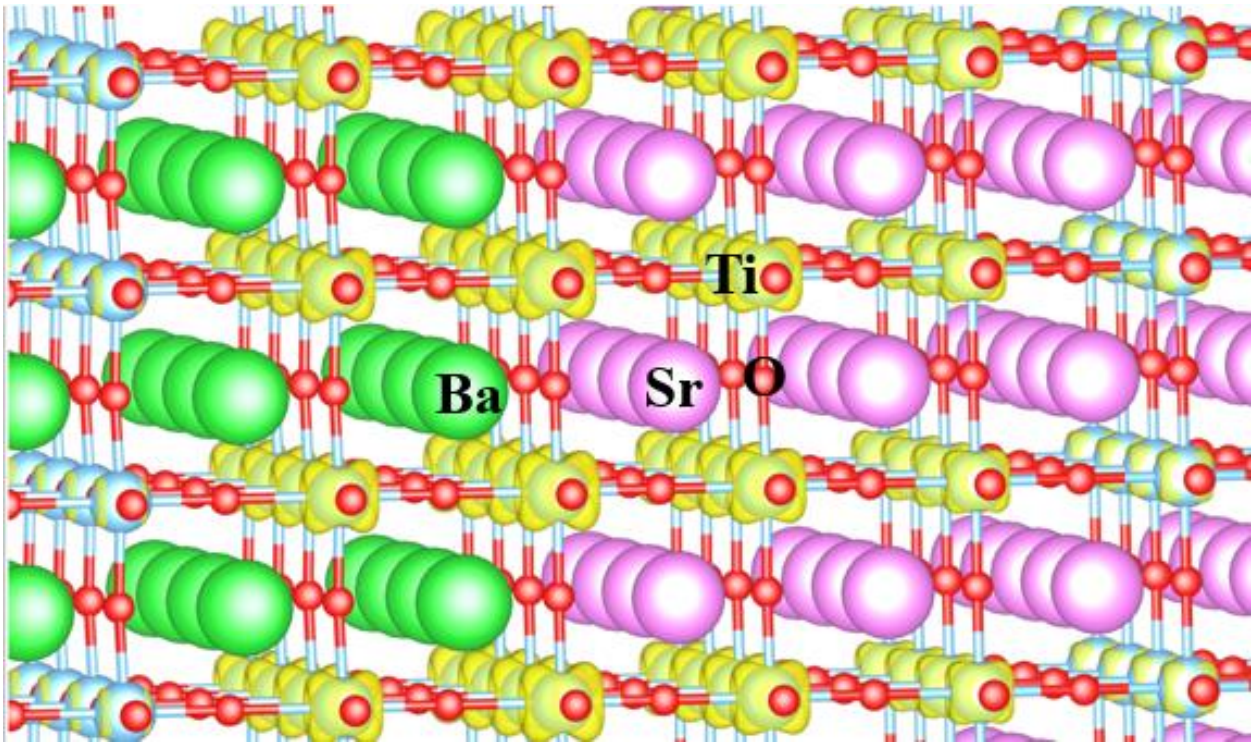
Ti
Ba
Sr
O

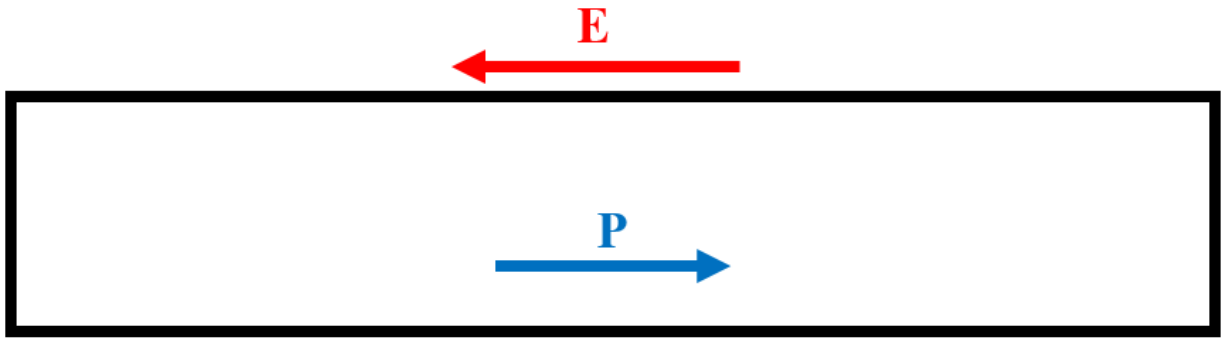
E
P

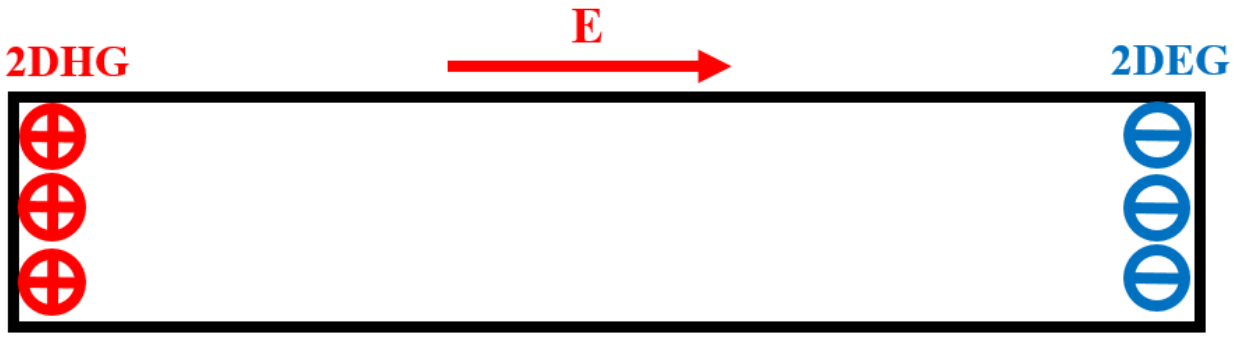
E
2DHG
2DEG